Research article

EFFECTS OF FILLING RATIO, ORIENTATION AND PRINT TEMPERATURE ON BENDING PROPERTIES OF 3D PRINTED PLA BEAMS

Önder Yeşil[1]* , Kemal Mazanoğlu[1]

[1]Usak University, Department of Mechanical Engineering, Usak, Turkey

Abstract

In this study, flexural properties of 3D printed PLA beam specimens produced with different filling ratios, orientations and print temperatures are experimentally investigated. Various bending specimens were produced by means of 3D printer using PLA filament as raw material. Low, intermediate and high filling ratios, lengthwise/widthwise and crosswise filling orientations, and different print temperatures were chosen as alternative production parameters of the printer. Manufactured beam specimens were subjected to three-point bending tests at room temperature in accordance with the TS EN ISO 178 standard. Effects of production parameters on mechanical bending properties including flexural modulus, maximum flexural stress, flexural strain at break, maximum force, and maximum deflection are clearly shown and discussed to state reasonable explanations of test results and to make conclusive suggestions.

Keywords: 3D printed PLA beams; flexural beam properties; filling ratio effects; orientation effects; temperature effects.

1. Introduction

Fused deposition modeling (FDM) is a production method that consists of melting, extruding and cooling steps conducted by the automated machines called 3D printers. In many applications, this method can be advantageous and more convenient than conventional manufacturing methods. 3D printer takes the thermoplastic filament, melts and extrudes it onto the plate and thus produces designed 3D model layer by layer from the bottom to top. Many engineering components may have complicated parts that can be

*Corresponding author: Önder Yeşil
E-mail: onder.yesil@usak.edu.tr

available to be produced by 3D printers. This easy production method can also play important role in research and development activities by reducing the cost consumed.

Plastic based materials such as ABS (Acrylonitrile butadiene styrene), PLA (Polylactic acid), and PA (Polyamide) have the common usage in 3D printing area because of their characteristic properties. Through them, PLA, which is biodegradable, has a lower melting temperature that makes it proper for many 3D printer systems. Engineers may have a question in their mind whether 3D printed materials have the sufficient strength to fulfill their tasks. In connection to the strength, mechanical parameters such as stress, strain, Young's modulus and etc. are frequently taken as key elements varying with filling ratio and filling orientation of 3D printed components. This work concentrates on such mechanical properties of beam type components in flexure.

Researchers have investigated the mechanical properties of 3D printed materials especially in recent years. They have considered tensile, compressive, and flexural properties. Hernandez et al. [1] state that filling orientation is the key point to achieve optimum functionality and proper mechanical properties in the additive manufacturing (AM) based elements. Cantrell et al. [2] investigate the mechanical properties of ABS and polycarbonate components produced by 3D printers. Their experimental characterization results obtained by means of digital image correlation (DIC) show that although orientation has minor effects on Young's modulus and Poisson's ratio of tensile specimens, it leads to variation of shear modulus and shear yield strength parameters up to 33%. Kim et al. [3] investigate tensile properties of 3D printed specimens made of single and dual materials to enhance those properties. They analyze influences of several experimental variables such as structural arrangement and material ratio of specimens. Christiyan et al. [4] reach to the conclusion that flexural strength properties of printed object made of PLA material are greatly influenced by layer thickness, printing speed, and orientation. Engkvist [5] presents a study on microstructural and mechanical properties of Nylon samples printed with various filling patterns. Letcher and Waytashek [6] present a study on the mechanical properties of PLA specimens printed with different orientations. Weng et al. [7] investigate the mechanical properties of 3D printed ABS/montmorillonite nanocomposite samples. Their experimental results show that the addition of 5% OMMT (organic modified montmorillonite) improves the tensile strength of 3D printed ABS samples. Dizon et al. [8] introduce a detailed overview on mechanical characterization of 3D printed polymers under different loading types such as tensile, bending, compressive, fatigue, impact and etc. Khuong et al. [9] inspect tensile and flexural strength parameters of ABS materials utilized in biomimetic robotic applications. They conclude that 3D printing technology can be an effective tool to simulate most of the biological structure. Stautner et al. [10] analyze the thermal and mechanical properties of selected 3D printed thermoplastics in the cryogenic temperature regime. They compile the information available and show a roadmap for designing additively manufactured components in cryogenic engineering. Wittbrodt and Pearce [11] perform X-ray diffraction (XRD) analyses to observe effects of print temperature and PLA color on material and mechanical properties of 3D printed components. According to their test results, percent crystallinity can either be minimum or maximum for white PLA extruded at different temperatures from 190 °C to 210 °C. They suggest that, in connection to the percent crystallinity, print temperature can be influential on the ultimate tensile strength of PLA specimens. Wu et al. [12] investigate the influence of layer thickness, filling orientation, deformation temperature and recovery temperature on shape recovery ratio and maximum shape recovery rate parameters of 3D printed PLA samples.

This paper shows an experimental study to explore effects of 3D printer production parameters on flexural strength parameters of PLA beams printed and tested in compliance with the relevant standard. Filling ratio, filling orientation, and print

temperature are examined as production parameters. To the best of authors' knowledge, this is one of the initial works to consider and scientifically explain the effects of filling parameters and print temperature on flexural properties of printed PLA beams.

Nomenclature

σ_f	: stress on fibers of elongated surface at the mid-point of the beam length (MPa)
M_z	: bending moment around the Z-axis (Nmm)
I_z	: area moment of inertia around the Z-axis (mm⁴)
y	: perpendicular distance to X-Z plane (mm)
F	: force applied from the mid-point of the beam specimen (N)
L	: support span (mm)
w	: width of the beam specimen (mm)
h	: thickness of the beam specimen (mm)
ε_f	: strain of elongated surface at the mid-point of the beam length, (mm/mm)
d	: deflection at the mid-point of the beam specimen (mm)
E_f	: flexural modulus of elasticity, (MPa)
$\dfrac{\Delta F}{\Delta d}$	: the gradient of the initial linear part of the load-deflection curve (N/mm)

2. Theoretical fundamentals

In this study, three-point bending tests are applied to all PLA specimens. Once force applied by the three-point bending test machine and dimensional parameters are known, relevant stress, strain, and modulus of elasticity parameters can be easily calculated by using following formulations:

$$\sigma_f = \frac{M_z}{I_z} y = \frac{3FL}{2wh^2} \tag{1}$$

$$\varepsilon_f = \frac{6dh}{L^2} \tag{2}$$

$$E_f = \frac{\sigma_{f2} - \sigma_{f1}}{\varepsilon_{f2} - \varepsilon_{f1}} = \frac{L^3}{4wh^3} \frac{\Delta F}{\Delta d} \tag{3}$$

Subscripts "1" and "2"denote certain values of stress and strain parameters.

## 3. Production and test conditions

3.1. Printer properties

3D printer in operation is on Cartesian type robotic system with moving nozzle in vertical plane and moving bed in remaining third coordinate perpendicular to the plane of nozzle motion. Printer was operated in print speed as 5 mm/s and such a low speed was selected to minimize production errors in printing. Retraction speed and print-free travel speed of nozzle were chosen as 25 mm/s. While diameter of PLA filament penetrating to nozzle was 1.75 mm, melted PLA extruded from the nozzle was much thinner since the diameter of the nozzle was designated as 0.4 mm. In addition, each layer of samples was printed with the

layer thickness, 0.2 mm. It is worth noting that, layer thickness is selected lower than the diameter of melt material flowing from the nozzle in order to provide adequate bonding forces between layers. Thickness of edge wall surrounding the inner pattern of the sample was selected as 0.8 mm, which should be same or multiple of nozzle diameter. Double of nozzle diameter was chosen as wall thickness in order to obtain considerable and measurable mechanical properties even if the sample has low filling ratio. Printing temperature was adjusted as 202 °C for the production of samples used to examine filling ratio and orientation parameters. Different print temperatures as 194 °C and 210 °C were also set to produce samples utilized in inspection of print temperature effects. For any set temperatures, however, some temperature deviations, ± 3 °C, could be rarely seen during the printing process. Raft layer option was selected to ensure bonding of samples onto the bed at the cost of consuming more material and time. Printing speed of raft layers was adjusted to 20 mm/s.

3.2. Production of test samples

PLA test specimens were produced at room temperature, 23 °C, and dimensioned as 4×10 mm^2 cross-section area and 80 mm length in compliance with the TS EN ISO 178 standard. Samples were printed with three different filling ratios adjusted in printer as 25%, 50%, 75% and two different inner pattern orientations designated in lengthwise/widthwise 0°/90° and crosswise +45°/-45° directions. Sample photos for each type of beam specimen are shown in Fig. 1. Although filling ratios were selected as noted above, actual filling ratio was slightly greater than these set up ratios. Because, melt material flowing with the diameter, 0.4 mm, was spread to the edges due to the printing with lower layer thickness, 0.2 mm. Net filament lengths and print durations varying with filling ratios are given in Table 1 that does not include the filament length, 0.61 m, and the time, 10 min, used up during the raft production standard for all types of beam specimens.
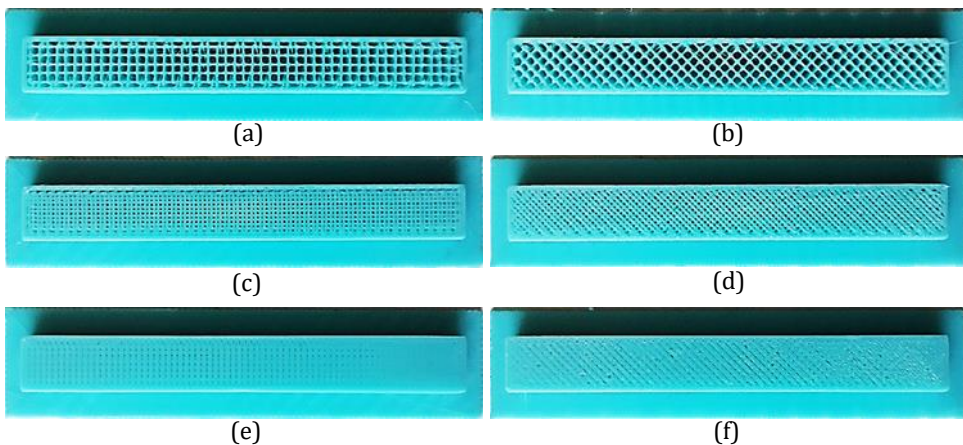
Fig. 1 Sample photos of (a) Type 1, (b) Type 4, (c) Type 2, (d) Type 5, (e) Type 3, and (f) Type 6 test specimens on their raft layers.

Five samples at least were manufactured for each type of specimen. Average mechanical properties were calculated from these samples, but, abnormal values largely deviating from others were eliminated in calculation. Thus, deviations that may be caused by the production errors were minimized.

Table 1 Set filling ratios, filament lengths and print durations of beam specimens.

Specimen type	Set filling ratio	Net filament length (m)	Net print duration (min)
1 and 4	25 %	0.51	53
2 and 5	50 %	0.79	81
3 and 6	75 %	1.07	109

3.3. Three-point bending test set-up

Three-point bending tests are carried out on tensile testing machines that apply increasing mid-point load to a specimen placed on two supports as schematized in Fig. 2. Test parameters can be determined according to standards (EN ISO 178, ASTM D790, EN ISO 14125, ASTM D2344 etc.) related to the three-point bending tests and plastic specimens. As noted before, EN ISO 178 standard, which is valid for thin plastic specimens, was used in this work. Relevant specimen dimensions were given in previous subsection. Distance between supporting points (L) was 64 mm as standardized value. Applied loads and corresponding deflections were simultaneously measured by means of a load cell and an extensometer mounted on the universal tensile testing machine giving results recorded by a computer. Test specimens were deflected with a constant rate (2 mm/min) until they were ruptured from their soffits. Fig. 3 shows sample photos of ruptured surfaces for each type of beam specimen. Note that fibers in white colors indicate regions exposed to high tensile stresses and strained during the bending. Conjectural borderlines between two colors, which are more obvious on side walls, can be the trace of approximate neutral axes of beams in bending where there are negligible elongation and compression. As can be understood from clarity or blurriness of photos in Fig. 3, samples filled in lengthwise/widthwise directions show almost planar fracturing behavior in contrast to the out planar fracturing behavior of samples with crosswise filling.
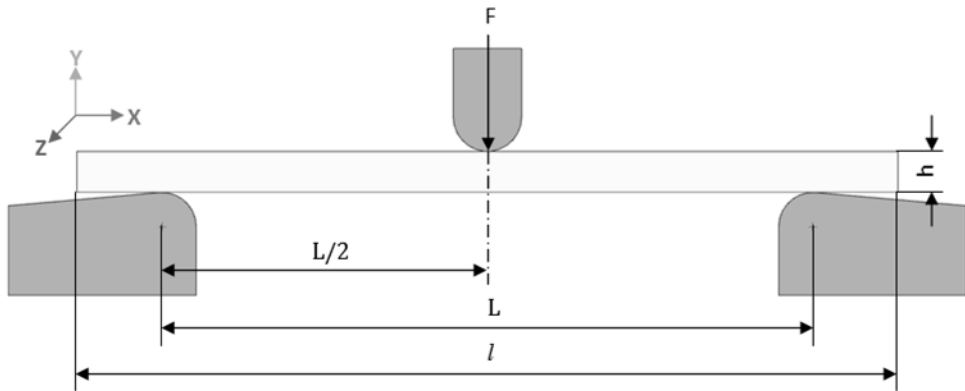
**Fig. 2** Schematic representation of three-point bending test set up.
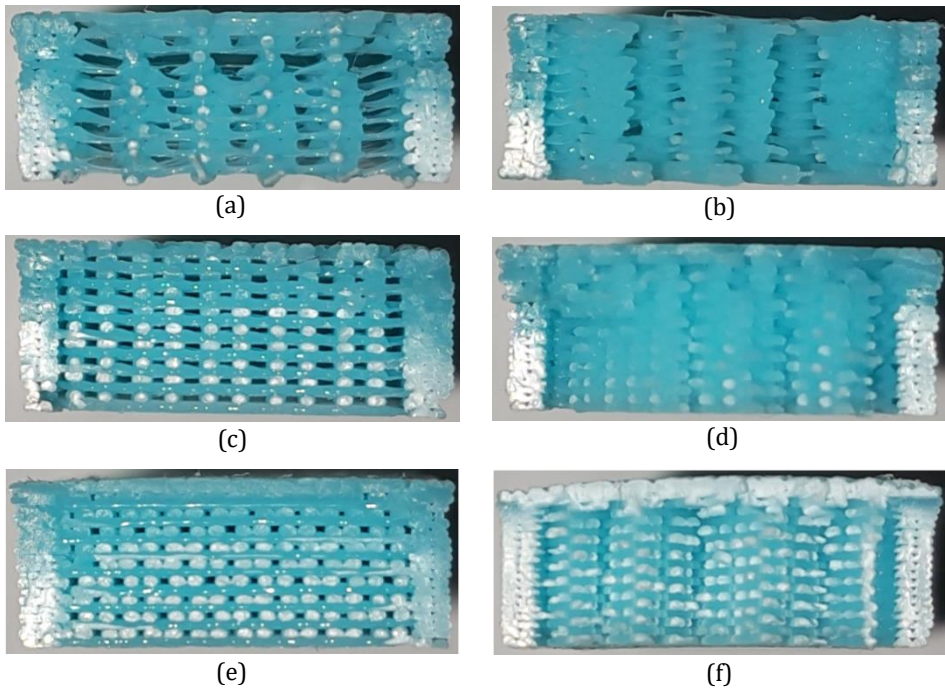
Fig. 3 Sample photos of ruptured surfaces after three-point bending tests applied to (a) Type 1, (b) Type 4, (c) Type 2, (d) Type 5, (e) Type 3, and (f) Type 6 beam specimens.

4. Results and discussion

In this section, results of three-point bending tests are analyzed in terms of mechanical bending properties. Although visual inspection of fractured surfaces shown in Fig. 3 gives a general idea about the result, it can be insufficient for many mechanical properties and misleading in demonstration of details due to non-scalable photographing effects such as lighting, shining, angles and etc. Therefore, further investigation is necessary to obtain more detailed, specific, and scalable results on beams tested. Mechanical bending parameters obtained as test results are tabulated in Table 2. In addition to this, resulting stress-strain graphs for all types of specimens produced with print temperature, 202 °C, are shown in Fig. 4.

Table 2 Mechanical bending properties of tested beam specimens with different filling ratios and filling orientations.

Orientation	Filling Ratio	Specimen Type	E_f (MPa)	σ_{fM} (MPa)	σ_{fB} (MPa)	ε_{fB} (%)	F_{max} (N)	d_{max} (mm)
0° / 90°	25 %	1	885	24.6	22.2	5.4	40.7	9.3
	50 %	2	1535	40.9	37.3	3.4	69.5	5.9
	75 %	3	2551	62.4	56.4	3.1	102.5	5.3
+45° / -45°	25 %	4	717	20.2	19	4.0	35.3	6.9
	50 %	5	1168	33.4	31.3	4.4	57	7.7
	75 %	6	2356	65.6	48.6	5.4	109.3	9.5
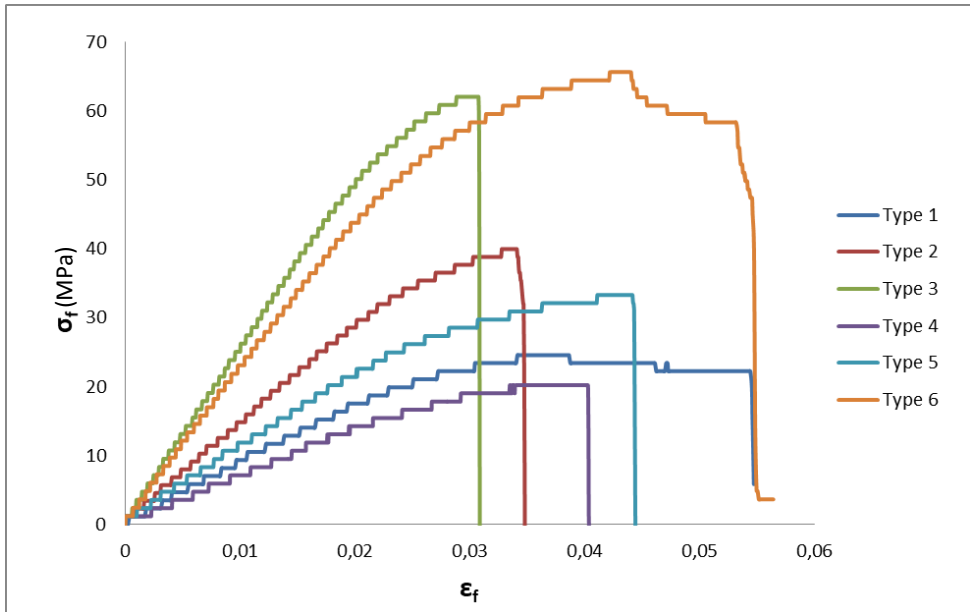
Fig. 4 Stress – strain diagrams for all specimen types produced with the print temperature, 202 °C.

As one expects, strain values linearly rise with increasing stresses at initial stages when the strain is lower than 0.02. However, linear parts of curves have different slopes that lead to different values of flexural modulus, E_f, proportional to bending stiffness. In terms of flexural modulus, maximum value is obtained for specimen type 3 with 0°/90° orientation and 75% filling ratio. On the other hand, specimen type 4 with +45º/−45º orientation and 25% filling ratio leads to minimum flexural modulus. Specimen type 6 with +45º/−45º orientation and 75% filling ratio reaches the largest values in terms of not only maximum flexural stress, σ_{fM}, but also flexural strain at break, ε_{fB}. Interestingly, specimen type 3 has minimum values of flexural strain at break although the same specimen type breaks at the largest level of stress called as flexural stress at break, σ_{fB}.

In a general aspect, maximum flexural stress, flexural stress at break and flexural modulus parameters increase with ascending filling ratio. This trend can be expected since higher filling ratios have larger bonding surfaces yielding higher total bonding forces between layers. Flexural strain at break parameter represents similar trend for only the orientation, +45º/−45º, while counter trend is remarkably followed for the orientation, 0º/90º. Combination of changes in parameters such as fiber lengths, contingence amount through fibers, stress distribution capability, and cooling speed should be effective on these notable results. As is known, larger deformability or less brittleness increase the deflection capacity of beams. Long and thin fibers spread throughout the length of beam specimens filled in the orientation, 0º/90º, contribute to the deformability in case of spaced filling but to the brittleness in case of intensive filling. Besides, intensive filling causes faster cooling and contributes to brittleness of the sample produced. For that reasons, spaced filling in the orientation, 0º/90º, yields beam specimens that are capable to distribute stress throughout the length of the beam and thus contributes to late fracture after large deflection. In case of spaced filling with the orientation +45º/−45º, however, deformability is lower due to short fibers ended at side walls and stresses are mainly distributed to side walls. Resulting localized stress and low deformability contributes to

early fractures at small deflections. When the filling ratios rise to 50 % and 75 %, stresses on fibers are easily transmitted to adjacent fibers due to intensive pattern formation. Therefore, as one expect, flexural strain and thus deflection capacity increases with ascending filling in the orientation, +45°/−45°.

When the orientation options are compared, it is generally seen that the orientation, 0°/90°, yields higher values of stresses and flexural modulus. This result is mainly caused by the stress distribution capability noted in previous paragraph. The orientation, 0°/90°, provides better distribution of stress throughout the length of beam and thus obtaining higher stress and modulus parameters. Variations of maximum force, F_{max}, and maximum deflection, d_{max} parameters resembles to those of maximum flexural stress and flexural strain at break parameters respectively since the stress is function of force and the strain is function of deflection as given in Eqs. (1) and (2).

Mechanical bending properties of Type 1 samples are also investigated in terms of the effects of different print temperatures. It is obtained that changes of print temperatures as 194 ℃, 202 ℃, and 210 ℃ have no clear effects on stress and flexural modulus parameters but lead to considerable deviations on strain parameters as given in Table 3 and shown in Fig. 5.

Table 3 Mechanical bending properties of Type 1 specimens produced with different print temperatures.

Print temperature	E_f (MPa)	σ_{fM} (MPa)	σ_{fB} (MPa)	ε_{fB} (%)	F_{max} (N)	d_{max} (mm)
194 ℃	910	25.0	21.2	3.8	40.0	6.7
202 ℃	885	24.6	22.2	5.4	40.7	9.3
210 ℃	912	24.0	22.6	3.5	37.6	6.4
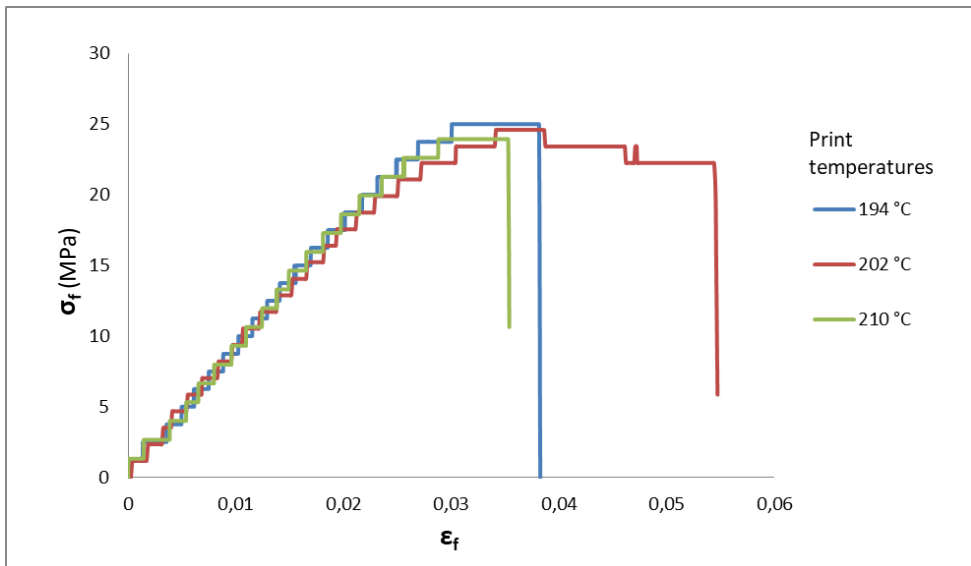
Fig. 5 Stress – strain diagrams of Type 1 samples produced with different print temperatures.

Strain at break values become highest and lowest when the print temperatures are 202 ℃ and 210 ℃ respectively. Print temperature of 194 ℃ gives rise to low-intermediate value of the strain at break parameter. This result can be found interesting but it can reasonably be explained. It should be kept in mind that PLA material does not melt under 180 ℃. In addition to this, temperature of extruded material is exponentially decaying based upon Newton's law of cooling. Material extruded with 210 ℃ cools faster than others and thus its temperature drops under 180 ℃ in a short duration. Fast cooling makes the sample less deformable and therefore, flexural strain at break values are lower than others when the print temperature is 210 ℃. On the other hand, when the sample produced using 194 ℃ as print temperature, extruded material temperature rapidly drops under melting temperature because of the small difference between the print and melting temperatures. In this case, extruded material becomes solid without forming maximum bonding forces between layers. It is for this reason that samples printed with 194 ℃ yield flexural strain at break values lower than those of samples printed with 202 ℃. Parallel to this result, it can be noticed from the Fig. 4 that extrusion conducted at 202 ℃ cause long non-linear stress–strain characteristics representing plastic deformations while vice versa is correct for other print temperatures.

5. Conclusions

This paper experimentally investigate the effects of filling ratio, filling orientation and print temperature parameters on mechanical bending properties of PLA beam specimens produced by 3D printer. It is worth noting that to investigate mechanical properties of 3D printed beams has recently attracted attention of engineering researchers. Furthermore, existing works generally consider the tensile properties of printed beams. This work contribute to current literature especially by analyzing the effects of filling parameters and print temperatures on bending properties of printed PLA beams. As a result of analyses discussed, conclusive remarks can be summarized as follow:

i. Higher flexural modulus, maximum force, and stress parameters can be reached with increasing filling ratio.
ii. Higher flexural strain and deflection capability can be obtained with more intensive crosswise filling on the contrary of lengthwise/widthwise filling.
iii. Lengthwise/widthwise filling can be more preferable than the crosswise filling if higher modulus, stress and strain parameters are needed with low filling ratios.
iv. In contrast to previous remark, crosswise filling can be more preferable than the lengthwise/widthwise one if higher modulus, stress and strain parameters are needed with high filling ratios.
v. Print temperature does not clearly effect the flexural modulus, stress and force parameters.
vi. For the PLA material, print temperature in the vicinity of 202 ℃ can be ideal to obtain more extensible samples at the cost of some plastic deformations seen at large deflections.

References

1. Hernandez R, Slaughter D, Whaley D, Tate J and Asiabanpour B. Analyzing the tensile, compressive, and flexural properties of 3D printed ABS P430 plastic based on printing orientation using fused deposition modeling. In: Bourell DL. Solid Freeform Fabrication 2016: Proceedings of the 26th Annual International Solid Freeform Fabrication Symposium – An Additive Manufacturing Conference; 2016 Aug 7-10; USA, Texas, Austin: The University of Texas at Austin; 2016. p. 939-950.

2. Cantrell J, Rohde S, Damiani D, Gurnani R, DiSandro L, Anton J, Young A, et al. Experimental characterization of the mechanical properties of 3D-printed ABS and polycarbonate parts. Rapid Prototyping Journal, 2017;23(4):811-824.
3. Kim H, Park E, Kim S, Park B, Kim N and Lee S. Experimental study on mechanical properties of single- and dual-material 3D printed products. Procedia Manufacturing, 2017;10:887-897.
4. Jaya Christiyan KG, Chandrasekhar U and Venkateswarlu K. Flexural properties of PLA components under various test condition manufactured by 3D printer. Journal of the Institution of Engineers (India) Series C, 2018;99(3):363-367.
5. Engkvist G. Investigation of microstructure and mechanical properties of 3D printed Nylon, MSc. Thesis, Lulea University of Technology, Lulea, Sweden, 2017.
6. Letcher T and Waytashek M. Material property testing of 3D printed specimen in PLA on an entry-level 3D printer. In: Pelegri A, Kardomateas G. Advanced Manufacturing: ASME International Mechanical Engineering Congress and Exposition (IMECE2014); 2014 Nov 14-20; Canada, Montreal: ASME Proceedings; 2014. p. V02AT02A014–8.
7. Weng Z, Wang J, Senthil T and Wu L. Mechanical and thermal properties of ABS-montmorillonite nanocomposites for fused deposition modeling 3D printing. Materials & Design, 2016;102:276-283.
8. Dizon JRC, Espera AH, Chen Q and Advincula RC. Mechanical characterization of 3D-printed polymers. Additive Manufacturing, 2018;20:44-67.
9. Khuong TL, Gang Z, Farid M, Yu R, Sun ZZ and Rizwan M. Tensile strength and flexural strength testing of acrylonitrile butadiene styrene (ABS) materials for biomimetic robotic applications. Journal of Biomimetics, Biomaterials and Biomedical Engineering, 2014;20:11-21.
10. Stautner W, Vanapalli S, Weiss KP, Chen R, Amm K, Budesheim E and Ricci J. The scope of additive manufacturing in cryogenics, component design, and applications. IOP Conference Series: Materials Science and Engineering, 2017;278(1):012134–11.
11. Wittbrodt B and Pearce JM. The effects of PLA color on material properties of 3-D printed components. Additive Manufacturing, 2015;8:110-116.
12. Wu W, Ye W, Wu Z, Geng P, Wang Y and Zhao J. Influence of layer thickness, raster angle, deformation temperature and recovery temperature on the shape memory effect of 3D-printed polylactic acid samples. Materials, 2017;10(8):970–16.